

Influence of Southern Oscillation on New Zealand Weather

Bret A. MULLAN

*New Zealand Meteorological Service
P.O. Box 722, Wellington - New Zealand*

ABSTRACT

The Southern Oscillation is known to have a significant effect on New Zealand weather. In general, during the negative (El Niño) phase of the Oscillation, New Zealand experiences an increased frequency of cold southwesterly airstreams that result in more rain in the southwest of the country, and dry conditions in the north and east. During the positive (La Niña) phase, there is a tendency for increased cyclonic activity in the North Tasman and more slow-moving or blocking anticyclones to the southeast of New Zealand. This results in frequent warm moist northerly or northeasterly airstreams over the country, with warmer than normal temperatures nationwide and wetter conditions in parts of the North Island exposed to these prevailing winds.

The pressure anomalies in the New Zealand region associated with extremes of the Southern Oscillation Index show some seasonal variation. The anomalies are also not entirely linear with respect to the value of the SOI. This paper examines differences between El Niño and La Niña conditions as they affect New Zealand, and then discusses the predicted and observed anomalies in New Zealand weather associated with the 1988/89 La Niña episode.

1. Introduction

Interest in the Southern Oscillation and its regional effects has been high since the 1972–73 El Niño event that devastated the Peruvian anchovy fisheries, and particularly intense since the dramatic 1982–83 episode. Although the existence of the Southern Oscillation (SO) has been known for many years (Walker, 1923), it took some time for the link between the SO and periodic ocean warming off the Peruvian coast to be appreciated. However, the term ENSO, for El Niño–Southern Oscillation, quickly became accepted. More recently, the term La Niña has become popular for describing the opposite extreme to El Niño conditions.

There is a considerable recent literature on regional weather changes associated with fluctuations in the Southern Oscillation. In the Australasian region, for example, McBride and Nicholls (1983) have examined seasonal relationships between Australian rainfall and the Southern Oscillation Index (SOI). Some of the lag correlations they found are sufficiently promising that the Australian Bureau of Meteorology plans to start issuing regular seasonal outlooks to the public from mid-1989 (National Climate Centre, 1988). Gordon (1985, 1986) discussed how the seasonal patterns of rainfall and temperature over New Zealand are related to the SOI. These relationships, along with further work, enabled the New Zealand Meteorological Service to make statements about the long-range weather prospects during the 1986–87 El Niño and the more recent 1988–89 La Niña.

A good start has thus been made to documenting general SO–weather relationships. However, much more attention now needs to be paid to the differences from one ENSO event to another: the reasons for the different evolution of the anomaly patterns, and the regional implications. This paper is a contribution to this need, essentially from a New Zealand point of view. Our particular interest is to examine anomalies associated with La Niña and El Niño, and see whether the anomalies vary linearly with the SOI. Predicted and observed anomalies in New Zealand during the 1988/89 La Niña summer are used as an example.

2. Data

The Southern Oscillation Index data used here cover the period May 1851 to December 1988. Parker's (1983) monthly values from January 1935 to March 1983 were updated using the standard 6-hourly pressure readings (at 0000, 0600, 1200 and 1800 GMT) at Tahiti and Darwin. The base period 1941–80 was used to normalize the Tahiti–Darwin pressure difference to form the so-called "Troup" Index (McBride and Nicholls, 1983). The SOI time series was extended back to 1851 using the seasonal Index values published by Wright (1975). Regression equations were calculated for each month of the year (N.D. Gordon, pers. comm.) relating the monthly Tahiti–Darwin pressure difference to Wright's Index values of the surrounding three seasons. The period 1935–1974 was used to generate the regression equations, which were then applied to Wright's values to extend the SOI time series back to 1851.

Although the basic SOI time series consists of monthly values, running three-monthly means are used throughout the analyses of this paper.

The pressure anomaly calculations (Section 4) use monthly mean sea level pressures determined from daily grid-point values on a 5° by 10° latitude–longitude grid over the New Zealand–Australia region (Gordon, 1986). These data cover the period July 1957 to September 1988. In the verification of the 1988–89 anomalies, the pressure time series was updated to February 1989 using the daily ECMWF analyses over the Southern Hemisphere from 20°S to 90°S that are received operationally by the New Zealand Meteorological Service. In addition, time series of monthly temperature and rainfall at selected New Zealand stations were used.

3. Persistence

a. SOI AUTOCORRELATION

The SOI time series shows considerable persistence from month to month. Conventional wisdom has it that the autocorrelation is highest during May–July and there is a "break" in persistence about March–April. Hence, Gordon (1986) recommended that the 12-month period May–April, rather than the calendar year, be used when calculating annually averaged relationships with the SOI. The break in persistence occurs because there is a tendency for new ENSO events to become established in May–June and also for existing events to weaken during February–March (at least in so far as ENSO behaviour is represented by the SOI).

Fig. 1 shows the seasonal variation in autocorrelation of the 3-month running mean SOI at lags up to 12 months. The lag autocorrelations were calculated separately according to whether the starting 3-month mean SOI was positive (1a) or negative (1b). Gordon (1986) calculated lag correlations that included all starting SOI values irrespective of sign, and his Fig. 2 is very similar to our Fig. 1b. It appears then that the autocorrelation structure of "all SOI" is dominated by that for "negative SOI" (Fig. 1b). The pattern for a starting "positive SOI" is somewhat different, with slightly greater persistence for starting months January–March and reduced persistence for the remainder of the year. The "positive SOI" result is also much noisier, particularly in March–May, the southern autumn, although the sample size is similar for each month (at slightly over 40% of the total).

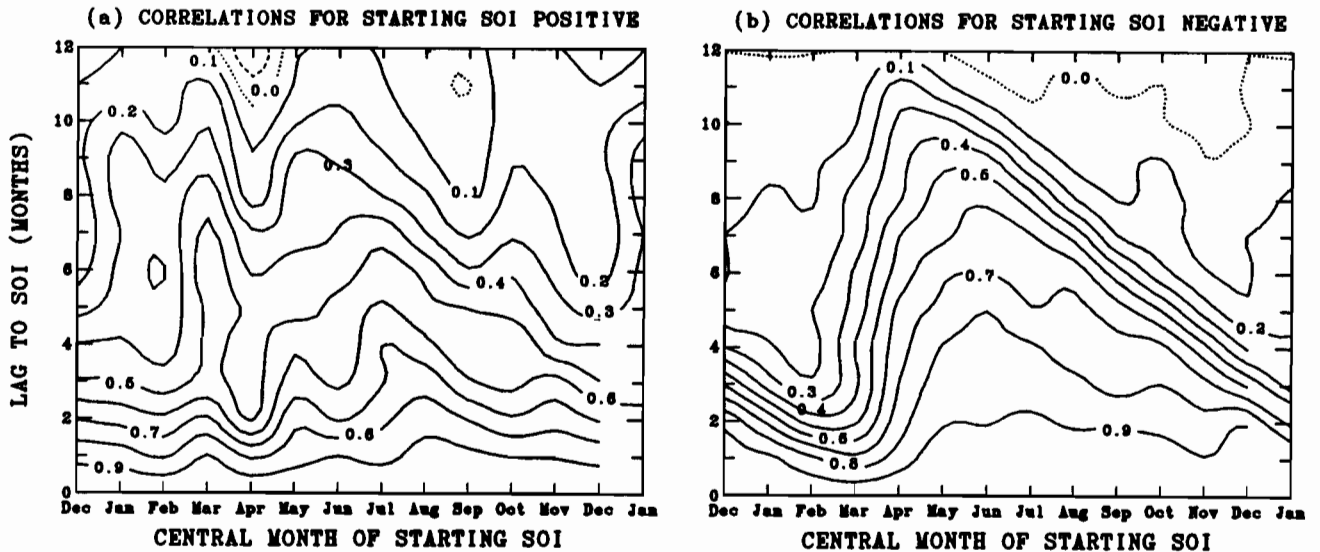


FIG. 1. SOI autocorrelation between the 3-month average centered on the given starting month and the 3-month average for 1–12 months later. Results cover the period May 1851 to December 1988 for 3-month average starting SOI positive (a), and for 3-month average starting SOI negative (b).

b. LA NIÑA/EL NIÑO EVENTS

In an attempt to identify further characteristics of La Niña and El Niño events, an objective definition of these events in terms of the SOI time series was applied. “Positive”/“negative” events (identified with La Niña/El Niño events, respectively) were defined to start when the 3-month running average SOI became at least S_0 above/below zero and remained that way for at least three consecutive months. The event continued until the 3-month running average SOI became smaller than S_1 above/below zero.

Various combinations of S_0 and S_1 were tried and the final values decided upon were $S_0 = 10$ and $S_1 = 5$ (in units of 0.1 standard deviation). The events identified by this choice agreed reasonably well with ENSO events identified by other authors (such as van Loon, 1984, and Rasmusson and Carpenter, 1982). Taking $S_1 = S_0$, for example, often resulted in breaking up what should have been single events into two or more parts.

Over the period of record, 11 positive (La Niña) events were identified, excluding the one apparently in progress in 1851 where the starting month could not be determined and the 1988–89 event that had not finished. The length varied from 10 to 23 months, with a mean of 14.0 months. Of the negative (El Niño) events, 29 were identified, of which 3 were of less than six-months duration (in 1857/58, 1957/58 and 1963/64). The length of the negative events varied from 3 to 47 months, with a mean of 13.7 months. Table 1 shows the distribution of the start and end months of the events selected. The reason for the seasonal break in persistence seen in Fig. 1 is quite obvious.

A relationship between the “intensity” of an event and its duration was also sought. Defining the starting intensity I_n of an event as the mean of the unsmoothed SOI values over the first n months, I_n was correlated against duration. While nothing useful was found for negative events, quite large correlations were found for positive events, which maximised at $n = 5$ ($r = +0.90$). Fig. 2 shows a scatter plot of La Niña starting intensity (average SOI over first 5 months) against duration.

TABLE 1. Start and end months of the 11 La Niña and 29 El Niño events identified in the period 1851–1988.

	J	F	M	A	M	J	J	A	S	O	N	D
Start month:												
<i>La Niña</i>	1	0	1	2	2	1	1	0	0	1	1	1
<i>El Niño</i>	1	3	3	7	2	1	3	3	1	2	1	3
End month:												
<i>La Niña</i>	1	2	1	2	0	0	0	0	2	1	1	1
<i>El Niño</i>	2	5	10	2	3	0	0	0	1	2	4	0

The 1988–89 La Niña event began strongly ($I_5 = 16.8$), and on the basis of Fig. 2 would be estimated to last for about 19–20 months from the start of August 1988; i.e., to about February–March 1990 before the 3-month running average SOI fell below +5. This prediction may not be too successful, as according to the latest observations (March 1989 Climate Diagnostics Bulletin) the current “cold episode conditions continued to show signs of weakening”. Various U.S. modellers (e.g., Cane and Barnett, as reported in *The New York Times*, 1989) also seem to agree that the current La Niña event should be over by mid-1989.

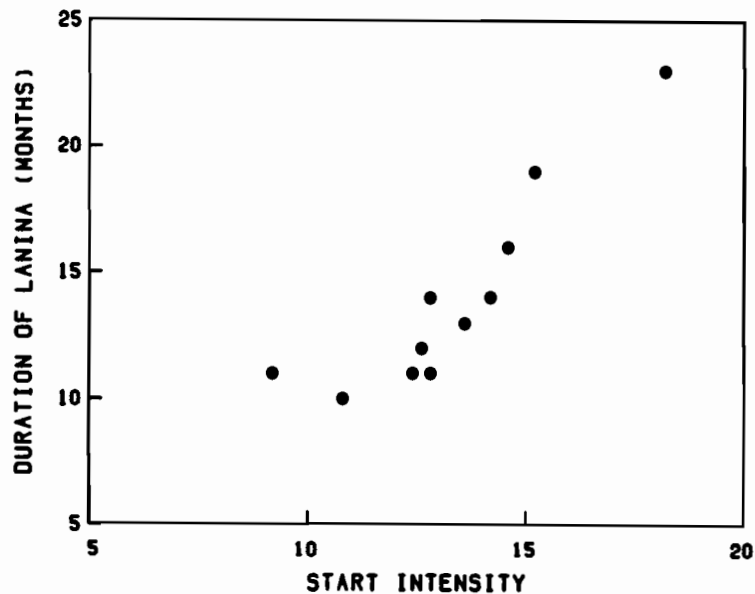


FIG. 2. Scatter plot of La Niña starting intensity (5-month average SOI, in units of 0.1 standard deviation) against calculated duration in months.

4. Pressure Anomaly Composites

a. METHOD

Gordon (1985,1986) calculated seasonal correlation maps of mean sea level pressure against SOI for an area covering Australia and New Zealand. Both positive and negative Index events were

included in the correlations. Overall, he found that positive SOI was associated with anomalous northeasterly flow over New Zealand (and, conversely, anomalous southwesterly flow during negative SOI periods). There was some seasonal variation in this pattern, with the flow anomalies displaying a more east/west direction in summer and more north/south in winter (for positive/negative SOI respectively).

In this section we will analyse the pressure variations not by a correlation pattern but by compositing seasonal pressure anomalies, weighted by the 3-month mean SOI for that season. Thus, if the array Y_i is the seasonal msl pressure anomaly over the Australia–New Zealand area, and x_i the seasonal SOI, we have:

$$Y_i = R x_i + C + E_i$$

where R is a “response” matrix, C a constant matrix, and E_i a random field for season i . Assuming that E_i has zero mean and is uncorrelated with the Index (i.e., $\bar{E}_i = 0$ and $\overline{x_i E_i} = 0$), we find:

$$R = \left(\frac{\overline{x_i Y_i} - \bar{x}_i \bar{Y}_i}{\overline{x_i^2} - \bar{x}_i^2} \right)$$

and $C = \bar{Y}_i - R \bar{x}_i$.

If the pressure field (Y_i) and SOI (x_i) time series were both normalised over the same base period as the composites are calculated for, then C would be zero. The pattern shown by the response matrix R is of course very similar to that of the correlation matrix. Thus, when displaying the pressure anomaly patterns associated with “all SOI”, it is equivalent to show either the correlation field (as in Gordon, 1986) or the predicted \hat{Y} (evaluated for some nominal Index value $x_i = 1$, say). Since our interest here is in the pressure pattern for subsets of the SOI data (in particular, positive and negative periods), it is more convenient to display the results in terms of the predictand \hat{Y} .

The significance of the resulting composite field was assessed by a Monte Carlo randomisation procedure. For the same season (e.g., summer) and period (1957–88) as the field in question, 1000 sets of composited response fields were calculated for randomly generated SOI series (with the same mean and standard as observed). The mean random response \bar{R} is essentially zero, but the standard deviation $S_{\bar{R}}$ of the random response allows us to calculate the significance of the initial composite. We thus normalise the composite by evaluating:

$$R_N = 100 \left(\frac{R - \bar{R}}{1.64 S_{\bar{R}}} \right)$$

Values of $|R_N|$ greater than 100 denote regions where the pressure response is significantly different from random at the 90% level (2-sided test).

b. RESULTS

Weighted composites of seasonal pressure anomaly fields were calculated for each season for three cases: using the whole sample regardless of the sign of the SOI (“all”), compositing only those seasons when the SOI was positive (“+”), and compositing only those seasons when the SOI was negative (“-”). The linearity of the pressure response with respect to the sign of the SOI could thus be assessed. Calculations showed that the linearity was good through December–May (Southern Hemisphere summer and autumn), but relatively poor in the June–November (winter and spring) period. Hence, using the seasonal correlation patterns of Gordon (1985,1986) to predict flow

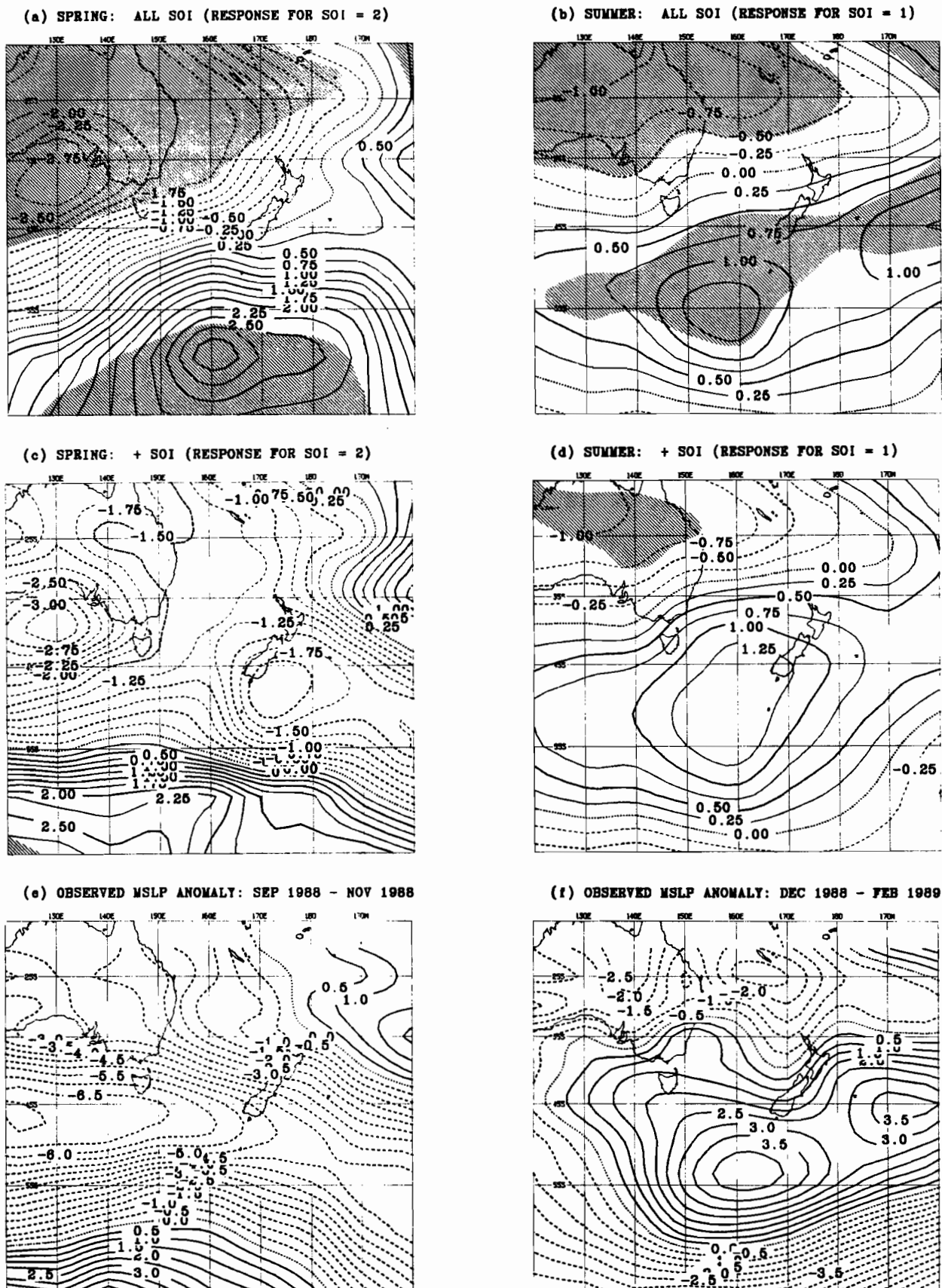


FIG. 3. Seasonal pressure anomaly patterns. Predicted anomaly, based on sample of "all" seasons, for a spring SOI of 20 (3a) and a summer SOI of 10 (3b). Predicted anomaly, based on sample of "+" SOI seasons, for a spring SOI of 2.0 (3c) and a summer SOI of 1.0 (3d). Observed anomaly for spring 1988 (3e), and for summer 1988/89 (3f). Shading indicates the composite response is significantly different from random at 90% level.

anomalies during both La Niña and El Niño periods could be expected to be reasonably successful in summer and autumn, but less so in winter and spring. Further discussion here is restricted to the spring (September–November) and summer (December–February) seasons.

Fig. 3 shows examples of calculated and observed seasonal pressure anomalies (in millibars) for the spring (Fig. 3a, c, e) and summer (Fig. 3b, d, f) seasons. The periods used to calculate the composites did not include the verification period September 1988–February 1989. The observed anomalies (Fig. 3e, f) cover a period of the current La Niña event. The 3-month running average SOI (Fig. 4) reached a maximum of 2.0 for the September–November (spring) 1988 period and decreased to an average of 1.1 over December–February (summer) 1988/89. (Note the change in contour interval from 0.25 mb in the composites to 0.50 mb in the observed fields.)

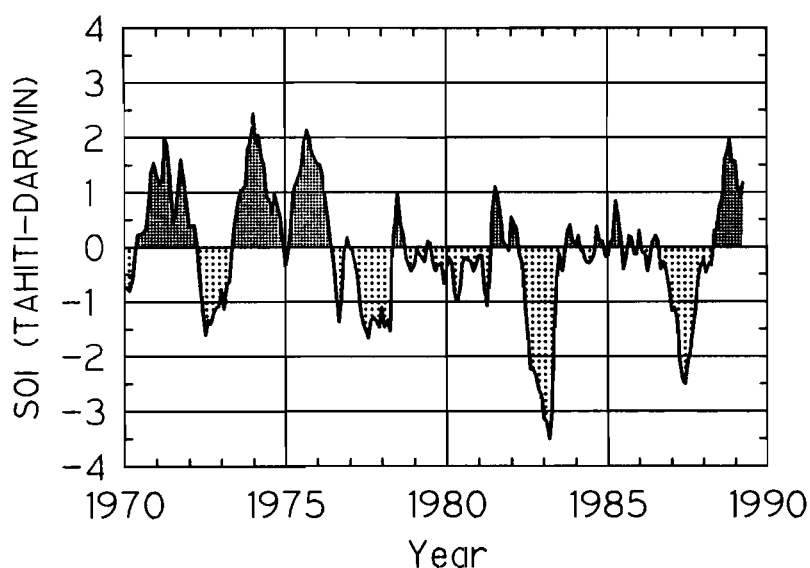


FIG. 4. Three-month running average SOI from January 1970 to April 1989 (in standard deviation units).

New Zealand was affected by stronger than normal westerlies throughout the 1988 winter and much of spring. This caused high rainfalls and some severe flooding on the west coast of the South Island, while drought conditions developed on the eastern side of the South Island mountain range. A sudden breakdown of the strong westerly flow occurred in early November, and a succession of persistent slow-moving anticyclones crossed the South Island during the summer, which served to further aggravate the drought there. Fig. 3e, f show the seasonal pressure anomaly patterns over this spring and summer period.

The predicted spring pressure anomaly, evaluated for the observed SOI of 2.0, is shown in Fig. 3a, c. It is clear that developing the composite using all spring seasons (Fig. 3a), and therefore the standard correlation approach too, completely fails to capture the stronger westerlies that affected New Zealand during the 1988 spring. The composite developed from only those spring seasons where the SOI was positive (Fig. 3c) is much more successful. Since Fig. 3c uses only about half the data set of Fig. 3a, the significance levels are lower, as indicated by the shading changes. The predicted summer pressure anomaly associated with Southern Oscillation changes is shown in Fig. 3b, d, evaluated for an SOI of 1.0, close to that observed. As mentioned above, the relationship between the flow anomaly over New Zealand and the SOI is more linear in summer than spring, so Fig. 3b, d are quite similar. The main difference is that in Fig. 3d the anticyclone is stronger and extends over more of the country.

5. 1988/89 Summer

The observed temperature and rainfall anomalies in New Zealand during the 1988/89 summer (December 1988–February 1989) are shown in Fig. 5a, b. The maps are based on daily temperature and rainfall observations from 46 stations evenly distributed around the country. Fig. 5c indicates the locations of places mentioned in the text. Temperatures were above normal over the whole country, with the largest anomalies occurring in the South Island and the southwestern half of the North Island. Rainfall was below normal in almost all eastern districts from Dunedin to East Cape.

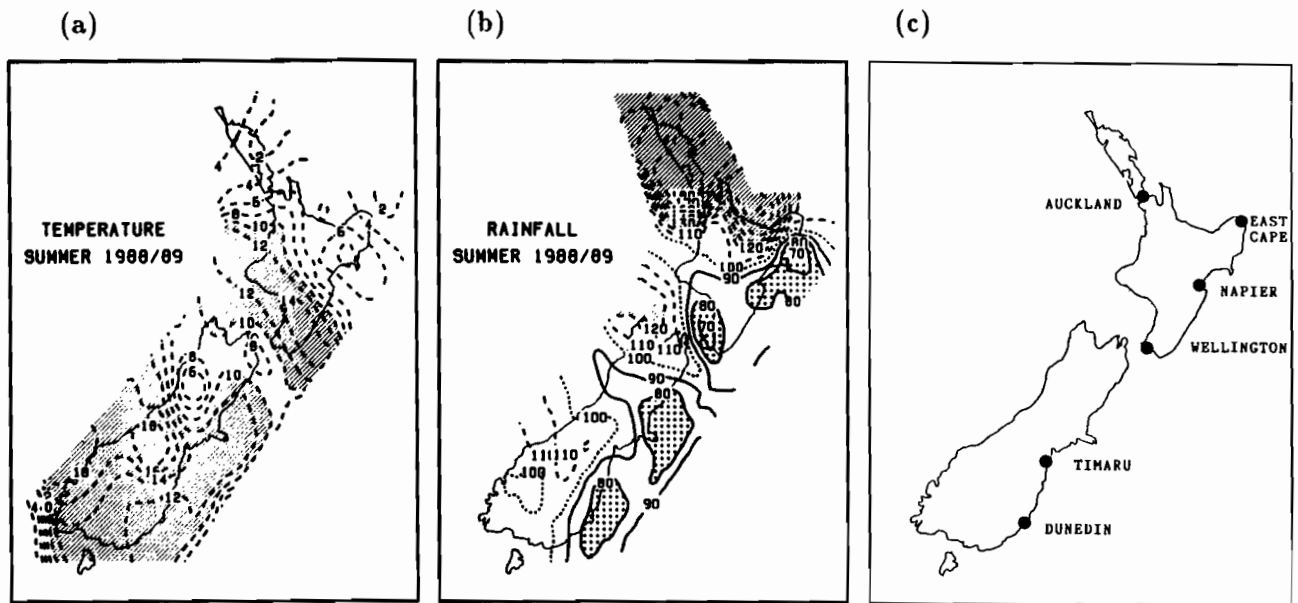


FIG. 5. Observed temperature anomalies (a, in 0.1°C) and rainfall (b, as % normal) over New Zealand during the 1988/89 summer season. Temperature anomalies greater than 1.0°C are shaded. Rainfall greater than 120% normal shaded and less than 80% stippled. (c) Map of New Zealand, showing some places mentioned in text.

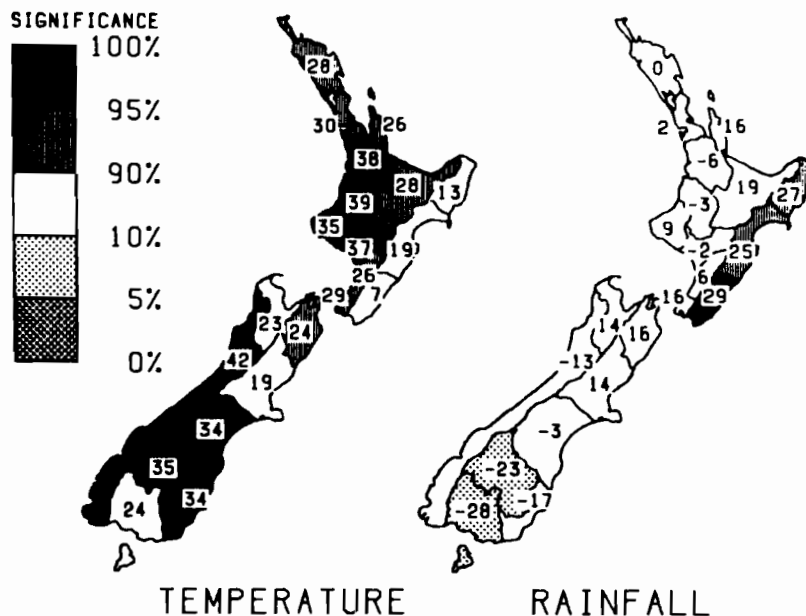


FIG. 6. Correlations ($\times 100$) between summer temperature and rainfall anomalies and the summer SOI, for various subregions of New Zealand. Significance levels indicated by shading (from Gordon, 1985).

Over the summer the drought that had previously affected only southeastern South Island areas extended up into eastern districts of the North Island as well. On the other hand, much above normal rainfall was experienced in the northern part of the North Island. Many places from Auckland northward received almost twice their normal summer rainfall. January was a particularly wet month, with rainfall in these northern areas being three to five times normal.

The pattern of temperature and rainfall anomalies over the country can be compared to the correlation patterns found by Gordon (1985), based on 30–34 years of data (Fig. 6). The main discrepancies with the observed patterns over the 1988/89 summer occur in the north and east of the North Island. In the north there was more rainfall, greater cloudiness and smaller (but still positive) temperatures anomalies than might have been anticipated. In the east of the North Island, rainfall was below normal (presumably as a result of the more intense anticyclonic anomaly over the country with a ridge extending up the east coast, Fig. 3f), and not above normal as Fig. 6 would indicate for significantly positive SOI.

6. Analogue Prediction

A comparison of Fig. 5 and Fig. 6 shows some features of (particularly) the rainfall distribution over New Zealand where the correlation pattern does not agree too well with that observed during the La Niña summer of 1988/89. Thus, we attempt again to separate the effects of La Niña and El Niño in the rainfall pattern as was done with the pressure anomaly. In this case, however, a somewhat different approach was taken: namely, the selection of analogues. (This analysis was actually done prior to the 1988/89 summer season, and was part of the background information used by the New Zealand Meteorological Service in issuing a long-range weather outlook for the summer on 19 October 1988.)

Analogues of 1988 were selected subjectively from examination of the 3-month running average SOI series. We selected La Niña start years (years zero, in the terminology of Rasmusson and Carpenter, 1982) to be those where the SOI rose from essentially zero at the beginning of the year to a positive value of at least one standard deviation above zero in the middle part of the year. Analogue years after 1900 were 1909, 1916, 1938, 1950, 1955, 1964, 1970, 1973, and 1975. Earlier events were not relevant since, in general, the station data sets do not extend back beyond the early years of the century. The only difference between this set of years and those chosen more objectively in Section 3b was the inclusion of 1964 which did not appear in the earlier set. The temperature and rainfall distribution during the winter and spring of year zero and during the following summer were then examined. Only the results for summer rainfall will be discussed here.

Monthly rainfall over the summer season at a number of representative long-record stations was allocated to categories of “dry”, “near normal” and “wet”, where for the examples shown here we take “near normal” to mean 81–119% of the normal monthly rainfall. Doing this for all years in the period of record, we could calculate an *a priori* probability that a summer month would be “dry” or “wet”. The actual number of “dry” and “wet” summer months for the La Niña analogue seasons were counted, and the binomial test applied to assess the significance of the result. Fig. 7 shows the result in histogram form for the stations of Auckland and Timaru.

The changed temperature and rainfall category distribution in La Niña analogue years generally supported the correlation maps shown in Fig. 6, although there were some differences. Fig. 7a gives a stronger indication than Fig. 6 of Auckland being wet during a La Niña summer, although the results do not quite come up to the 90% significance level. (For example, the *a priori* probability of

a “dry” summer month in Auckland is $p = 0.460$, but during past analogue La Niña summers only 9 of 27 months have been “dry”, which has a probability of 0.13 of occurring by the binomial test.) The analogue approach also predicted the east coast of the North Island (Napier, not shown) should not be as dry in La Niña summers as “all” summers, a result that supports Fig. 6 but conflicts with the observations (Fig. 5b).

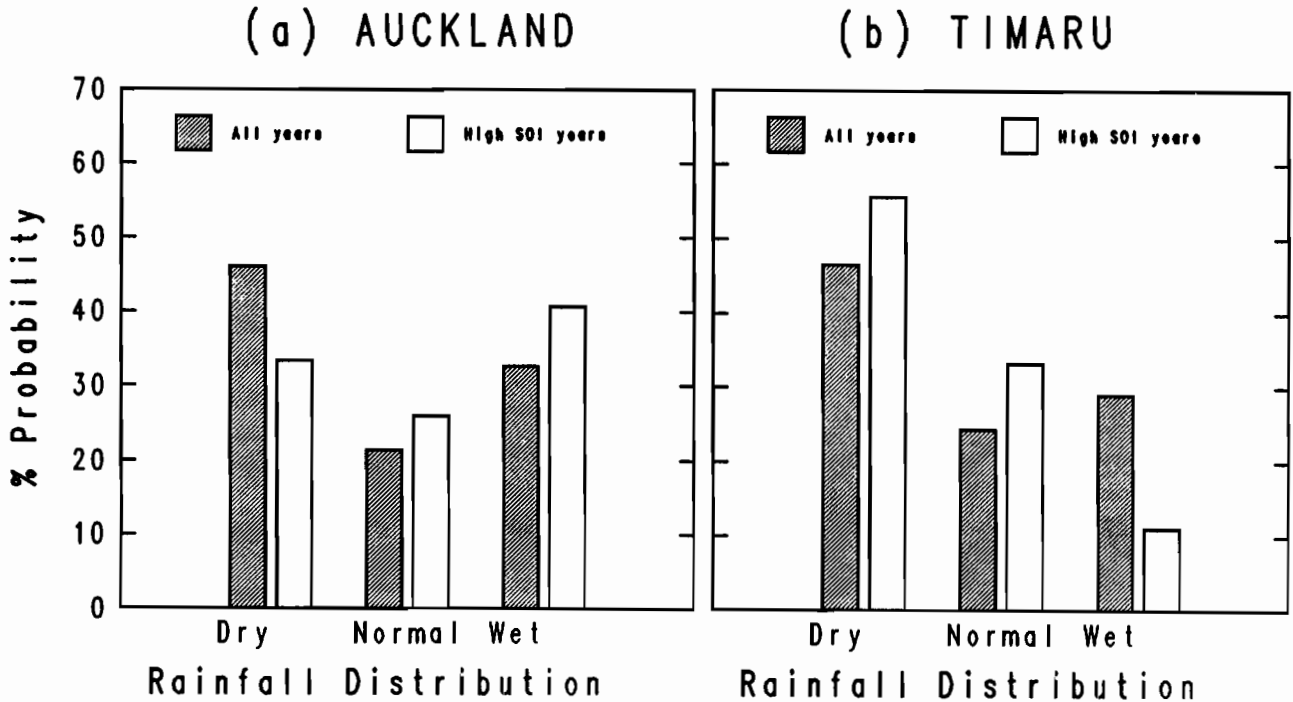


FIG. 7. Probability of Auckland (a) and Timaru (b) rainfall falling into one of three categories, comparing all years of record with La Niña analogue years.

7. Conclusions

Although New Zealand is not near the centres of action of the Southern Oscillation, it is nevertheless affected by this phenomenon. Significant anomalies in the seasonal pressure distribution around New Zealand do occur, and these result in temperature and rainfall anomalies over the country. The general pattern of the anomalies and their seasonal variation have been documented previously in terms of correlation maps. This procedure implicitly assumes a linearity of the response to the forcing.

We have shown that this assumption of linearity is not always valid. In particular, over the period September–November 1988 when the SOI reached a positive extreme, it seems necessary to take account of *nonlinearity* in the response in order to explain the observed pressure distribution. The summer case is not as obvious although, even here when the SOI value was less extreme, there was some improvement in the predicted anomalies using only that part of the historical record when the SOI was positive.

Acknowledgments

The extended SOI series and Fig. 6 was provided by Neil Gordon. I would also like to thank John Marsh, Director of International TOGA Project Office, for financial assistance that made possible my participation in the Noumea TOGA Conference.

REFERENCES

- Gordon, N.D., 1985: The Southern Oscillation: a New Zealand perspective. *J. Royal Soc. of New Zealand* 15: 137–155.
- Gordon, N.D., 1986: The Southern Oscillation and New Zealand weather. *Mon. Wea. Rev.* 114: 371–387.
- McBride, J.L., and Nicholls, N., 1983: Seasonal relationships between Australian rainfall and the Southern Oscillation. *Mon. Wea. Rev.* 111: 1998–2004.
- National Climate Centre, 1988: Seasonal outlooks (Based on El Niño/Southern Oscillation (ENSO) Relationships). Australian Bureau of Meteorology, August 1988, 46 p.
- Parker, D.E., 1983: Documentation of a Southern Oscillation index. *Meteor. Mag.*, 112: 184–188.
- Rasmusson, E.M., and Carpenter, T.H., 1982: Variations in tropical sea surface temperature and surface wind fields associated with the Southern Oscillation/El Niño. *Mon. Wea. Rev.*, 110: 354–384.
- The New York Times, 1989: *Science Times*, Tuesday, January 3, 1989.
- van Loon, H., 1984: The Southern Oscillation. Part III: Associations with the trades and with the trough in the westerlies of the South Pacific Ocean. *Mon. Wea. Rev.*, 112: 947–954.
- U.S. Dept. of Commerce, 1989: Climate Diagnostics Bulletin. March 1989. Climate Analysis Center, Washington.
- Walker, G.T., 1923: Correlation in seasonal variations of weather, VIII. *Mem. Indian Meteor. Dept.* 24: 75–131.
- Wright, P.B., 1975: An index of the Southern Oscillation. Climatic Research Unit Rep., CRU RP4, University of East Anglia, Norwich, NR4 7TJ, England, 22 pp.

**WESTERN PACIFIC INTERNATIONAL MEETING
AND WORKSHOP ON TOGA COARE**

Nouméa, New Caledonia

May 24-30, 1989

PROCEEDINGS

edited by

Joël Picaut *

Roger Lukas **

Thierry Delcroix *

* ORSTOM, Nouméa, New Caledonia

** JIMAR, University of Hawaii, U.S.A.

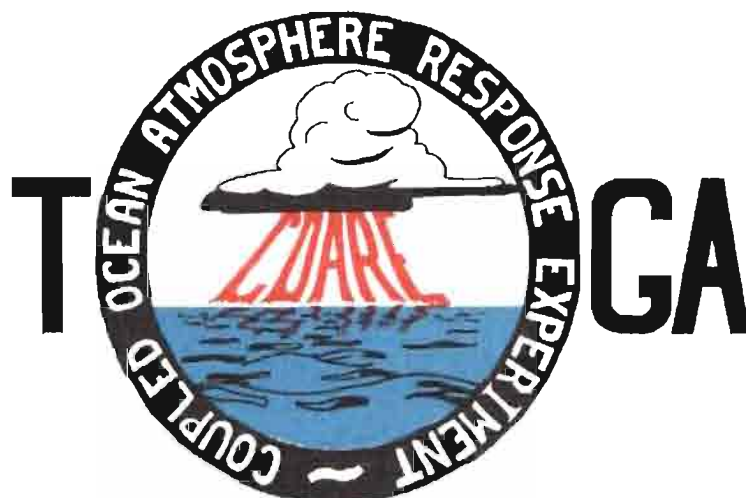


TABLE OF CONTENTS

ABSTRACT	i
RESUME	iii
ACKNOWLEDGMENTS	vi
INTRODUCTION	
1. Motivation	1
2. Structure	2
LIST OF PARTICIPANTS	5
AGENDA	7
WORKSHOP REPORT	
1. Introduction	19
2. Working group discussions, recommendations, and plans	20
a. Air-Sea Fluxes and Boundary Layer Processes	20
b. Regional Scale Atmospheric Circulation and Waves	24
c. Regional Scale Oceanic Circulation and Waves	30
3. Related programs	35
a. NASA Ocean Processes and Satellite Missions	35
b. Tropical Rainfall Measuring Mission	37
c. Typhoon Motion Program	39
d. World Ocean Circulation Experiment	39
4. Presentations on related technology	40
5. National reports	40
6. Meeting of the International Ad Hoc Committee on TOGA COARE	40
APPENDIX: WORKSHOP RELATED PAPERS	
Robert A. Weller and David S. Hosom: Improved Meteorological Measurements from Buoys and Ships for the World Ocean Circulation Experiment	45
Peter H. Hildebrand: Flux Measurement using Aircraft and Radars	57
Walter F. Dabberdt, Hale Cole, K. Gage, W. Ecklund and W.L. Smith: Determination of Boundary-Layer Fluxes with an Integrated Sounding System	81

MEETING COLLECTED PAPERS

WATER MASSES, SEA SURFACE TOPOGRAPHY, AND CIRCULATION

Klaus Wyrtki: Some Thoughts about the West Pacific Warm Pool	99
Jean René Donguy, Gary Meyers, and Eric Lindstrom: Comparison of the Results of two West Pacific Oceanographic Expeditions FOC (1971) and WEPOCS (1985-86)	111
Dunxin Hu, and Maochang Cui: The Western Boundary Current in the Far Western Pacific Ocean	123
Peter Hacker, Eric Firing, Roger Lukas, Philipp L. Richardson, and Curtis A. Collins: Observations of the Low-latitude Western Boundary Circulation in the Pacific during WEPOCS III	135
Stephen P. Murray, John Kindle, Dharma Arief, and Harley Hurlburt: Comparison of Observations and Numerical Model Results in the Indonesian Throughflow Region	145
Christian Henin: Thermohaline Structure Variability along 165°E in the Western Tropical Pacific Ocean (January 1984 - January 1989)	155
David J. Webb, and Brian A. King: Preliminary Results from Charles Darwin Cruise 34A in the Western Equatorial Pacific	165
Warren B. White, Nicholas Graham, and Chang-Kou Tai: Reflection of Annual Rossby Waves at The Maritime Western Boundary of the Tropical Pacific	173
William S. Kessler: Observations of Long Rossby Waves in the Northern Tropical Pacific	185
Eric Firing, and Jiang Songnian: Variable Currents in the Western Pacific Measured During the US/PRC Bilateral Air-Sea Interaction Program and WEPOCS	205
John S. Godfrey, and A. Weaver: Why are there Such Strong Steric Height Gradients off Western Australia ?	215
John M. Toole, R.C. Millard, Z. Wang, and S. Pu: Observations of the Pacific North Equatorial Current Bifurcation at the Philippine Coast	223

EL NINO/SOUTHERN OSCILLATION 1986-87

Gary Meyers, Rick Bailey, Eric Lindstrom, and Helen Phillips: Air/Sea Interaction in the Western Tropical Pacific Ocean during 1982/83 and 1986/87	229
Laury Miller, and Robert Cheney: GEOSAT Observations of Sea Level in the Tropical Pacific and Indian Oceans during the 1986-87 El Nino Event	247
Thierry Delcroix, Gérard Eldin, and Joël Picaut: GEOSAT Sea Level Anomalies in the Western Equatorial Pacific during the 1986-87 El Nino, Elucidated as Equatorial Kelvin and Rossby Waves	259
Gérard Eldin, and Thierry Delcroix: Vertical Thermal Structure Variability along 165°E during the 1986-87 ENSO Event	269
Michael J. McPhaden: On the Relationship between Winds and Upper Ocean Temperature Variability in the Western Equatorial Pacific	283

John S. Godfrey, K. Ridgway, Gary Meyers, and Rick Bailey: Sea Level and Thermal Response to the 1986-87 ENSO Event in the Far Western Pacific	291
Joël Picaut, Bruno Camusat, Thierry Delcroix, Michael J. McPhaden, and Antonio J. Busalacchi: Surface Equatorial Flow Anomalies in the Pacific Ocean during the 1986-87 ENSO using GEOSAT Altimeter Data	301

THEORETICAL AND MODELING STUDIES OF ENSO AND RELATED PROCESSES

Julian P. McCreary, Jr.: An Overview of Coupled Ocean-Atmosphere Models of El Nino and the Southern Oscillation	313
Kensuke Takeuchi: On Warm Rossby Waves and their Relations to ENSO Events	329
Yves du Penhoat, and Mark A. Cane: Effect of Low Latitude Western Boundary Gaps on the Reflection of Equatorial Motions	335
Harley Hurlburt, John Kindle, E. Joseph Metzger, and Alan Wallcraft: Results from a Global Ocean Model in the Western Tropical Pacific	343
John C. Kindle, Harley E. Hurlburt, and E. Joseph Metzger: On the Seasonal and Interannual Variability of the Pacific to Indian Ocean Throughflow	355
Antonio J. Busalacchi, Michael J. McPhaden, Joël Picaut, and Scott Springer: Uncertainties in Tropical Pacific Ocean Simulations: The Seasonal and Interannual Sea Level Response to Three Analyses of the Surface Wind Field	367
Stephen E. Zebiak: Intraseasonal Variability - A Critical Component of ENSO ?	379
Akimasa Sumi: Behavior of Convective Activity over the "Jovian-type" Aqua-Planet Experiments	389
Ka-Ming Lau: Dynamics of Multi-Scale Interactions Relevant to ENSO	397
Pecheng C. Chu and Roland W. Garwood, Jr.: Hydrological Effects on the Air-Ocean Coupled System	407
Sam F. Iacobellis, and Richard C.J. Somerville: A one Dimensional Coupled Air-Sea Model for Diagnostic Studies during TOGA-COARE	419
Allan J. Clarke: On the Reflection and Transmission of Low Frequency Energy at the Irregular Western Pacific Ocean Boundary - a Preliminary Report	423
Roland W. Garwood, Jr., Pecheng C. Chu, Peter Muller, and Niklas Schneider: Equatorial Entrainment Zone : the Diurnal Cycle	435
Peter R. Gent: A New Ocean GCM for Tropical Ocean and ENSO Studies	445
Wasito Hadi, and Nuraini: The Steady State Response of Indonesian Sea to a Steady Wind Field	451
Pedro Ripa: Instability Conditions and Energetics in the Equatorial Pacific	457
Lewis M. Rothstein: Mixed Layer Modelling in the Western Equatorial Pacific Ocean	465
Neville R. Smith: An Oceanic Subsurface Thermal Analysis Scheme with Objective Quality Control	475
Duane E. Stevens, Qi Hu, Graeme Stephens, and David Randall: The hydrological Cycle of the Intraseasonal Oscillation	485
Peter J. Webster, Hai-Ru Chang, and Chidong Zhang: Transmission Characteristics of the Dynamic Response to Episodic Forcing in the Warm Pool Regions of the Tropical Oceans	493

MOMENTUM, HEAT, AND MOISTURE FLUXES BETWEEN ATMOSPHERE AND OCEAN

W. Timothy Liu: An Overview of Bulk Parametrization and Remote Sensing of Latent Heat Flux in the Tropical Ocean	513
E. Frank Bradley, Peter A. Coppin, and John S. Godfrey: Measurements of Heat and Moisture Fluxes from the Western Tropical Pacific Ocean	523
Richard W. Reynolds, and Ants Leetmaa: Evaluation of NMC's Operational Surface Fluxes in the Tropical Pacific	535
Stanley P. Hayes, Michael J. McPhaden, John M. Wallace, and Joël Picaut: The Influence of Sea-Surface Temperature on Surface Wind in the Equatorial Pacific Ocean	543
T.D. Keenan, and Richard E. Carbone: A Preliminary Morphology of Precipitation Systems In Tropical Northern Australia	549
Phillip A. Arkin: Estimation of Large-Scale Oceanic Rainfall for TOGA	561
Catherine Gautier, and Robert Frouin: Surface Radiation Processes in the Tropical Pacific	571
Thierry Delcroix, and Christian Henin: Mechanisms of Subsurface Thermal Structure and Sea Surface Thermo-Haline Variabilities in the South Western Tropical Pacific during 1979-85 - A Preliminary Report	581
Greg. J. Holland, T.D. Keenan, and M.J. Manton: Observations from the Maritime Continent : Darwin, Australia	591
Roger Lukas: Observations of Air-Sea Interactions in the Western Pacific Warm Pool during WEPOCS	599
M. Nunez, and K. Michael: Satellite Derivation of Ocean-Atmosphere Heat Fluxes in a Tropical Environment	611

EMPIRICAL STUDIES OF ENSO AND SHORT-TERM CLIMATE VARIABILITY

Klaus M. Weickmann: Convection and Circulation Anomalies over the Oceanic Warm Pool during 1981-1982	623
Claire Perigaud: Instability Waves in the Tropical Pacific Observed with GEOSAT	637
Ryuichi Kawamura: Intraseasonal and Interannual Modes of Atmosphere-Ocean System Over the Tropical Western Pacific	649
David Gutzler, and Tamara M. Wood: Observed Structure of Convective Anomalies	659
Siri Jodha Khalsa: Remote Sensing of Atmospheric Thermodynamics in the Tropics	665
Bingrong Xu: Some Features of the Western Tropical Pacific: Surface Wind Field and its Influence on the Upper Ocean Thermal Structure	677
Bret A. Mullan: Influence of Southern Oscillation on New Zealand Weather	687
Kenneth S. Gage, Ben Basley, Warner Ecklund, D.A. Carter, and John R. McAfee: Wind Profiler Related Research in the Tropical Pacific	699
John Joseph Bates: Signature of a West Wind Convective Event in SSM/I Data	711
David S. Gutzler: Seasonal and Interannual Variability of the Madden-Julian Oscillation	723
Marie-Hélène Radenac: Fine Structure Variability in the Equatorial Western Pacific Ocean	735
George C. Reid, Kenneth S. Gage, and John R. McAfee: The Climatology of the Western Tropical Pacific: Analysis of the Radiosonde Data Base	741

Chung-Hsiung Sui, and Ka-Ming Lau: Multi-Scale Processes in the Equatorial Western Pacific	747
Stephen E. Zebiak: Diagnostic Studies of Pacific Surface Winds	757

MISCELLANEOUS

Rick J. Bailey, Helene E. Phillips, and Gary Meyers: Relevance to TOGA of Systematic XBT Errors	775
Jean Blanchot, Robert Le Borgne, Aubert Le Bouteiller, and Martine Rodier: ENSO Events and Consequences on Nutrient, Planktonic Biomass, and Production in the Western Tropical Pacific Ocean	785
Yves Dandonneau: Abnormal Bloom of Phytoplankton around 10°N in the Western Pacific during the 1982-83 ENSO	791
Cécile Dupouy: Sea Surface Chlorophyll Concentration in the South Western Tropical Pacific, as seen from NIMBUS Coastal Zone Color Scanner from 1979 to 1984 (New Caledonia and Vanuatu)	803
Michael Szabados, and Darren Wright: Field Evaluation of Real-Time XBT Systems	811
Pierre Rual: For a Better XBT Bathy-Message: Onboard Quality Control, plus a New Data Reduction Method	823